**Naval Research Laboratory**

**Monterey, CA 93943-5502**

**NRL/MR/7531--16-9693**

# NAVGEM Forecast and Observation Impact Experiments with Assimilation of ECWMF Analysis Data in the Global Domain

Brett T. Hoover
*University of Wisconsin–Madison*
*Madison, Wisconsin*

Rolf H. Langland
*Atmospheric Dynamics and Prediction Branch*
*Marine Meteorology Division*

September 22, 2016

# REPORT DOCUMENTATION PAGE

*Form Approved*
*OMB No. 0704-0188*



| **1. REPORT DATE** *(DD-MM-YYYY)* | **2. REPORT TYPE** | **3. DATES COVERED** *(From - To)* |
|---|---|---|
| 22-09-2016 | Memorandum Report | May 2015 – May 2016 |

**4. TITLE AND SUBTITLE**

NAVGEM Forecast and Observation Impact Experiments with Assimilation of ECWMF Analysis Data in the Global Domain

**5a. CONTRACT NUMBER**

**5b. GRANT NUMBER**

**5c. PROGRAM ELEMENT NUMBER**
PE: 0602435N

**6. AUTHOR(S)**

Brett T. Hoover* and Rolf H. Langland

**5d. PROJECT NUMBER**

**5e. TASK NUMBER**

**5f. WORK UNIT NUMBER**
75-1E82-A-6-5

**7. PERFORMING ORGANIZATION NAME(S) AND ADDRESS(ES)**

Naval Research Laboratory
Marine Meteorology Division, Code 7531
7 Grace Hopper Avenue
Monterey, CA 93943-5502

**8. PERFORMING ORGANIZATION REPORT NUMBER**

NRL/MR/7531--16-9693

**9. SPONSORING / MONITORING AGENCY NAME(S) AND ADDRESS(ES)**

Office of Naval Research
875 N. Randolph Street, Suite 1425
Arlington, VA 22203-1995

**10. SPONSOR / MONITOR'S ACRONYM(S)**

ONR

**11. SPONSOR / MONITOR'S REPORT NUMBER(S)**

**12. DISTRIBUTION / AVAILABILITY STATEMENT**

Approved for public release; distribution is unlimited.

**13. SUPPLEMENTARY NOTES**

*University of Wisconsin–Madison, Cooperative Institute for Meteorological Satellite Studies (CIMSS), Madison, WI 53706

**14. ABSTRACT**

The analyses, forecasts, and adjoint-derived estimates of observation-impact are compared between a control simulation of NAVGEM and simulations that include assimilation of wind and temperature "pseudo-raob" profiles derived from the ECMWF analysis, representing a synthetic dataset of high-quality observations. Assimilation of these pseudo-raob profiles, in this experimental context, improves NAVGEM forecast skill and reduces temperature and height biases in NAVGEM analyses and forecasts, particularly in southern hemisphere high-latitudes, where radiance observations are the predominate type of regular observation data. Assimilation of pseudo-raob observations reduces the impact of regular in situ and satellite observation types. However, with improvement of forecasts and analyses, there is a reduction in total observation-impact through convergence of the background and analysis state trajectories.

**15. SUBJECT TERMS**

Observation impact
Analysis uncertainty
Data assimilation
Adjoint model

| **16. SECURITY CLASSIFICATION OF:** | | | **17. LIMITATION OF ABSTRACT** | **18. NUMBER OF PAGES** | **19a. NAME OF RESPONSIBLE PERSON** |
|---|---|---|---|---|---|
| **a. REPORT** | **b. ABSTRACT** | **c. THIS PAGE** | | | Rolf Langland |
| Unclassified Unlimited | Unclassified Unlimited | Unclassified Unlimited | Unclassified Unlimited | 37 | **19b. TELEPHONE NUMBER** *(include area code)* (831) 656-4786 |

**Standard Form 298 (Rev. 8-98)**
**Prescribed by ANSI Std. Z39.18**

# 1. Introduction

The assimilation of new high-quality observation information in an analysis and forecast system can translate to significant changes in the analysis, the forecast, and impact of other observations. However, interaction between new observations and forecast improvement can be complex; for example, the introduction of high-quality observations can reduce bias in a short forecast that defines the model background into which observations are assimilated, thus reducing background error and also reducing the impact of observations in future analyses.

In this study, the Naval Research Laboratory's global spectral model and its four-dimensional variational (4D-VAR) data assimilation system are used to assimilate synthetic "observations" derived from analysis profiles of the European Center for Medium-Range Weather Forecasting (ECMWF), simulating a dataset of high-quality "pseudo-raob" observations. In this context, "pseudo-raobs" are defined as vertical profiles of wind and temperature derived from gridded analyses fields of the ECMWF model and interpolated onto a one-degree latitude longitude grid for assimilation into NAVDAS-AR.

Differences in analyses, forecasts and observation-impact between experiments and control are examined to identify which components of the regular global satellite and in-situ observing network are most and least affected by assimilation of pseudo-raobs. Systematic differences between experiment and control analyses help to identify and quantify possible biases in the control. Experiments are performed to investigate possible sources of bias in the control analysis at high southern hemispheric latitudes, and the extent to which these biases are corrected by pseudo-raob assimilation. An adjoint-based

Manuscript approved May 26, 2016.

observation-impact adjoint technique (Langland and Baker 2004) is used to calculate the impact on 24 hr forecast error from pseudo-raob observations and all regular observing.

The model and design of pseudo-raob experiments are defined in Section 2. In Section 3, design and results from the three pseudo-raob assimilation experiments are described in detail. Conclusions are provided in Section 4.

## 2. Experimental Design and Methodology

*2.1) Control Simulation*

The Navy Global Environmental Model (NAVGEM) is a semi-lagrangian version of the Navy Operational Global Atmospheric Prediction System (NOGAPS; Hogan and Rosmond 1991), run at T359 spectral resolution with 50 vertical levels. The NRL Atmospheric Variational Data Assimilation System- Accelerated-Representer (NAVDAS-AR; Xu et al. 2005) is a 4-dimensional variational data assimilation system including the adjoint of the NOGAPS model (Rosmond 1997), with an observation-space representation of the 4D-VAR algorithm (Rosmond and Xu 2006).

The NAVGEM control simulation and three experiments are initialized with identical initial conditions at the first analysis time, followed by a 6-hr analysis-forecast cycle that produces atmospheric analyses at 0000 UTC, 0600 UTC, 1200 UTC and 1800 UTC, with 120-hr forecasts started from initial conditions at 0000 UTC and 1200 UTC. The Control is cycled from 0000 UTC 20 April 2013 to 1200 UTC 6 June 2013[1]. Two

[1] The NAVGEM continues cycling beyond this time for the purposes of producing statistics on forecast skill out to 120 hrs validating against the NAVGEM analysis, but for the purposes of evaluating analyses and forecasts, the period of focus is 0000 UTC 20 April 2013 – 1200 UTC 06 June 2013.

experiments are then cycled over this same time period, while a third experiment is cycled only over a portion in the second-half of this period (see Section 2c).

The Control and all experiments use identical sets of satellite and in-situ observations, as per NAVGEM operations, aside from the assimilation of pseudo-raob observations. Approximately 2.6 million observations are ingested by NAVDAS-AR at each analysis time. The observation types, their names as they appear henceforth in figures and discussion of results, and the variables observed by each type are available in Table 1.

*2.2) Derivation of Psuedo-Raob Observations*

Three experiments in this study involve assimilation into NAVGEM of so-called "pseudo-raob" profiles derived from analysis fields of the ECMWF Integrated Forecast System (IFS), made available through the THORPEX Integrated Grand Global Ensemble (TIGGE) archive[2]. Analysis zonal wind (u), meridional wind (v), and temperature (T) grids are available every 0000 UTC and 1200 UTC at eight standard tropospheric pressure levels (1000, 925, 850, 700, 500, 300, 250, and 200 hPa) at one-half-degree resolution. Pseudo-raobs are assimilated in the NAVGEM on a one-degree resolution grid equatorward of 85 degrees latitude, totaling 1,477,440 pseudo-raob observations in a given 0000 UTC or 1200 UTC analysis-period. Of these available pseudo-raobs, typically about 90% are assimilated, the remainder being rejected in quality control.

Since they are obtained from analyses of a high-resolution, very accurate assimilation system (ECWMF), the assimilation of these pseudo-raob profiles have the

[2] http://apps.ecmwf.int/datasets/data/tigge

potential to improve the NAVGEM forecast to a greater extent than assimilation of regular satellite or in-situ data in NAVGEM. In addition, the assimilation of analysis-state profiles from ECMWF provides information that is independent of existing biases in the NAVGEM analysis and model background state. Note that since NAVDAS-AR uses a 6-hr data assimilation window, pseudo-raobs are not assimilated at 0600 UTC or 1800 UTC.

As will be shown, assimilation of pseudo-raobs is an effective method to smoothly draw the analyses and forecasts of one model (here, NAVGEM) closer to the state of another model (here, ECWMF). In theory, assimilation of "pseudo-raob" observations from any source should be beneficial, as long as the pseudo-raobs are more accurate than the background state of the model into which the pseudo-raobs are assimilated. This condition is exceeded in the current study, since ECMWF analyses are demonstrably more accurate than the 6-hr NAVGEM forecast which defines the NAVGEM model background.

*2.3) Experiments with Assimilation of Psuedo-Raob Observations*

In the first experiment (UVTOBS), the complete global dataset of ECMWF zonal wind, meridional wind, and temperature pseudo-raobs is assimilated at 0000 UTC and 1200 UTC, comprising nearly 1.5 million observations per 0000/1200 UTC analysis-period. This experiment quantifies the impact of assimilating both wind and temperature pseudo-raob profiles during the entire experiment period, while the next two experiments (TOBS and DIEOFF) quantify impacts from smaller subsets of pseudo-raob observations.

In the second experiment (TOBS), the experiment in UVTOBS is repeated, but only pseudo-raob temperature profiles are assimilated, comprising nearly half a million observations per 0000/1200 UTC analysis-period. A goal of this experiment is to study how the addition of high-quality temperature observations may affect the forecast impact of routinely assimilated wind observations such as polar Atmospheric Motion Vectors (AMVs). In particular, we wish to determine if a reduction of temperature bias in the NAVGEM background at polar latitudes influences assimilation of regular high-latitude wind observations, possibly through thermal wind balance.

In the third experiment (DIEOFF), pseudo-raob observations are assimilated as in UVTOBS for the first 96 analysis cycles of the experiment, after which no pseudo-raob observations are assimilated for the final 87 analysis cycles, covering the period from 0000 UTC 14 May 2013 – 1200 UTC 4 June 2013. It is this final 87 analysis cycle period over which the analysis/forecast system is evaluated in DIEOFF. The purpose of this experiment is to quantify the longer-term residual effects on analyses and forecasts that may persist from assimilation of pseudo-raob observations at earlier times. In particular, we wish to determine if assimilation of ECMWF pseudo-raobs for some finite period of time might provide a persisting bias-correction for later NAVGEM analyses and forecasts. In Control and all three experiments, forecast skill is evaluated using self-analysis, meaning that each simulation uses its own cycled analyses for verification.

*2.4) Adjoint estimate of observation impact*

Adjoint versions of the data assimilation system and forecast model are used to quantify the impact of all assimilated observations on short-range forecast error,

following the method of Langland and Baker (2004), which uses energy-based error-norms of forecasts on analysis and background trajectories. Formally, the impact of observations assimilated at an analysis time ($t_a$) producing an analysis state ($\mathbf{X}_a$), on the forecast at time $t_f = t_a + 24$ hr, is defined as the difference between (i) an error-norm $e(\mathbf{X}_{f,a})$ at $t_f$ of a forecast initialized from $\mathbf{X}_a$ and (ii) an error norm $e(\mathbf{X}_{f,b})$ at $t_f$ initialized from $\mathbf{X}_b$ , which is the background state used in the assimilation that produces $\mathbf{X}_a$ . In practice it is most efficient to compute $e(\mathbf{X}_{f,b})$ by extending the regular background forecast to 30 hr and directly computing the error norm from that forecast. Note that observation impact is zero if no observations are assimilated, in which case $\mathbf{X}_a = \mathbf{X}_b$. This form of observation impact diagnostic is part of routine monitoring for NAVGEM and has been used in the ECMWF global model (Cardinali 2009), and the GEOS-5 global model (Zhu and Gelaro 2008, Gelaro et al. 2010).

# 3. Results

*3.1) UVTOBS Experiment*

Mean analysis fields are computed for all 0000 UTC, 0600 UTC, 1200 UTC, and 1800 UTC analysis-periods from 0000 UTC 20 April 2013 to 1200 UTC 6 June 2013 for UVTOBS and the Control. Differences in the mean analysis between UVTOBS and Control show that assimilation of ECMWF analysis winds and temperatures in the form of pseudo-raobs produces a mean reduction of NAVGEM 500 hPa geopotential height globally, with largest height reductions in the southern hemisphere high latitudes (Fig. 1a). The largest reduction in mean 500 hPa geopotential height is roughly 20.4 m near 60°S and 60°E. The smallest mean change in 500 hPa analysis heights is found over the

continental United States, Europe, and China (shading in Fig.1a), where in-situ observation networks are robust and analysis uncertainty is generally low in operational analyses (Langland et al. 2008).

Reduction of mean 500 hPa geopotential heights in the analysis is consistent with reduced mean temperatures in the low to mid troposphere (Fig. 1b). The analysis zonal-mean temperature is cooled from the surface to 500 hPa across most of the globe, with the most cooling between 60S to 70S. Modest warming of the analysis appears in the upper troposphere and lower stratosphere, as well in the lower troposphere right over the North Pole. These changes to analysis zonal temperatures increase the meridional temperature and height gradient in the southern hemisphere between 45S and 60S, with a slight increase in speed of the southern hemispheric polar jet core (about +0.45 m $s^{-1}$ at 300 hPa at latitude of 55°S, black contours in Fig. 1b).

The analysis changes from assimilation of pseudo-raobs in this experiment produce NAVGEM forecast improvement across the global domain. Root-mean-squared error (RMSE) in geopotential height is reduced in UVTOBS compared to Control at all forecast times out to 120 hr and throughout the depth of the troposophere (Fig. 2). The largest improvements in geopotential height RMSE occur in the southern hemisphere near the tropopause, with smaller height forecast improvements in the northern hemisphere (Fig. 2a,b). Improvements in mean geopotential height RMSE are 1-4 m in the northern hemisphere and 1-7 m in the southern hemisphere, with improvements statistically significant at 95% confidence from 0-72 hr in the northern hemisphere and from 0-96 hr in the southern hemisphere. Forecast wind speed RMSE in the tropics is

improved as well, with mean error reductions of 0.66 m $s^{-1}$ at 500 hPa in 48hr forecasts (Fig. 2c).

The beneficial effect of pseudo-raob assimilation on NAVGEM forecasts is also shown by substantial reduction in the global energy-weighted error-norms for 24 hr and 30 hr forecasts. The error-norm is computed globally as total moist energy in the difference between the forecast state and a verifying analysis; the verifying analysis is obtained from the analysis/forecast system such that UVTOBS and the Control forecasts are each verified against their own analyses. In every instance, except the first few forecasts, the error-norm for both 24 hr and 30 hr forecasts is substantially lower in UVTOBS than in Control (Fig. 3a). The "saw-tooth" up and down pattern of the error-norm time-series in UVTOBS is caused by assimilation of ECMWF pseudo-raobs at 0000 UTC and 1200 UTC, although the 0600 UTC and 1800 UTC UVTOBS forecasts also produce lower error-norms than Control, due to information passed from pseudo-raobs through background forecasts used for the data assimilation.

Examination of the 24 hr and 30 hr error norms also reveals that assimilation of pseudo-raobs has *reduced* the NAVGEM total observation-impact, since the reduction in the 30 hr error norm ($e(\mathbf{X}_{f,b})$, error of forecasts on the background trajectories) has been reduced by a greater amount than the 24 hr error norm ($e(\mathbf{X}_{f,a})$, error of forecasts on the analysis trajectories). Specifically, the total observation impact in UVTOBS is reduced by about 15.6 percent from -7.77 J $kg^{-1}$ to -6.56 J $kg^{-1}$, as quantified by error of the nonlinear forecasts. The NAVGEM adjoint system is able to estimate the true nonlinear total observation impact with an accuracy of about 90 percent.

We note that reduction of total observation impact indicates an overall improvement of the forecast/analysis system, in which more-accurate background forecasts require smaller adjustments for each analysis. In other words, the addition of highly accurate observation information (e.g. pseudo-raob profiles) brings the background and analysis trajectories closer together at analysis time and in the forecast. In a hypothetical system with perfect analyses and forecasts, the observation impact would be zero, with no adjustments required for the background trajectory. Thus, incremental reduction of observation impact in an experiment is a reliable indicator of an improved system.

While the total observation-impact at the 24 hr range is reduced in UVTOBS, this reduction is not evenly distributed across all assimilated observation categories, as shown by adjoint-based estimates of observation impact, discussed below. For the NAVGEM Control, the largest reductions in NAVGEM 24 hr forecast error are associated with atmospheric motion vectors (AMVs) derived from geostationary satellite imagery (CLOUD_WIND), radiosonde observations (RADIOSONDE), and brightness temperature (radiance) observations from SSM/I, IASI, and AMSU-A (Fig. 4a).

When ECMWF pseudo-raobs are assimilated in UVTOBS, they become the dominant contributor to total observation impact in NAVGEM (providing 53.5% of the total mean observation-impact), while the impact of all other observation types is reduced to varying extents (Fig. 4a). The largest *total reduction* in observation impact occurs in CLD-WIND data, while largest *percentage-reductions* in impact occur in high-latitude satellite-derived wind observations from polar-orbiting satellites (AVHRR-WIND, MODIS-WIND, and LEO-GEO-WIND) and surface winds from SSM/I, WSAT, and

ASCAT. Recall that the high southern latitudes are also where assimilation of pseudo-raobs produces the largest reductions in NAVGEM 500 hPa geopotential height, coincident with maximum cooling in the low to mid troposphere (Fig. 1).

Impact from most routinely assimilated observation types is generally reduced in UVTOBS by 50 percent or more, compared to impacts in CONTROL (Fig. 4b). Moisture observations, including satellite-derived total precipitable water (TPW) data lose only about 10% of their impact (Fig. 4b), likely because no ECMWF analysis moisture pseudo-raobs are assimilated in the UVTOBS experiment. Impact of synthetic tropical cyclone observations (TC-Synth; Goerss and Jeffries 1994) reverses in sign (represented as a greater than 100% change in impact), although its total impact is very small.

The operational NAVGEM atmospheric analysis in southern hemispheric high-latitudes is primarily constrained by radiance and satellite wind observations, since the in-situ observation network is sparse. Differences between the UVTOBS and Control mean analysis temperatures suggest that the NAVGEM Control analysis is biased warm, particularly in high latitudes. Radiance observation data assimilated at these latitudes are not effective at removing bias from the background, since the radiance "bias correction" is calculated with reference to the background, assumed to be itself un-biased (Derber and Wu 1998, Harris and Kelly 2001).

The UVTOBS experiment shows that analysis bias is reduced by assimilation of ECMWF temperature and wind pseudo-raobs over the global domain. In the following experiment (TOBS) we assimilate temperature-only (excluding wind data) ECMWF pseudo-raob profiles to study how NAVGEM analyses and forecasts are affected by assimilation of this smaller subset of pseudo-raob information.

*3.2) TOBS Experiment*

In this experiment, with the addition of only ECMWF pseudo-raob temperatures (not winds) assimilated, the changes to mean analysis temperature in NAVGEM are similar to that observed for UVTOBS, with similar cooling through the lower to mid-troposphere and warming aloft (Fig. 5b). The changes to the mean 500 hPa geopotential height field are likewise similar, with lowering of heights globally, and the largest reduction in height occurring at high latitudes in the southern hemisphere (Fig. 5a), although the impact on the height field is slightly reduced in TOBS compared to UVTOBS. However, the mean speed of the southern hemispheric polar jet does not increase in TOBS as in UVTOBS (Fig. 5b); the additional lowering of heights poleward of the southern hemispheric polar jet in UVTOBS that is not seen in TOBS therefore may be a response to the ECMWF pseudo-raob wind observations increasing the speed of the jet.

Improvement in TOBS forecasts to 120 hrs has a similar pattern to that produced in UVTOBS, but with smaller-magnitude forecast differences and fewer statistically significant NAVGEM forecast improvements. Maximum improvement (3.5 m) in geopotential height RMSE occurs near tropopause-level in the southern hemisphere, with improvements in the northern hemisphere of smaller magnitude (maximum 2.3 m) (Fig. 6). In general, the magnitude of height RMSE improvement in TOBS is roughly 50-60 percent of that found in UVTOBS (Fig. 2), while improvement of wind errors in the tropics in TOBS is nearly neutral vs. Control. These scores imply that a significant fraction of height improvement in UVTOBS can be attributed to assimilation of just the

ECMWF pseudo-raob temperature observations, although without also including pseudo-raob wind observations these improvements are less statistically significant.

In terms of 24 hr and 30 hr forecast error-norms, TOBS provides a small fraction of the error reduction obtained in UVTOBS (Fig. 7). On average, 11.7 percent (16.7 percent) of the observed reduction in 24 hr (30 hr) error-norm in UVTOBS is retained in TOBS. In TOBS (as in UVTOBS) the 30 hr error-norm is reduced by a larger amount than the 24 hr error-norm, resulting in reduction of total observation-impact, although the reduction in TOBS is about 32% that obtained in UVTOBS.

While the effects on NAVGEM analyses and forecasts from pseudo-raobs in TOBS is smaller than in UVTOBS, there are similar patterns: (1) assimilating pseudo-raob data cools analysis temperatures and lowers analysis geopotential heights globally in the low to mid-troposphere, with largest cooling and lowering of heights at high latitudes in the southern hemisphere, (2) forecast skill scores are improved through 120 hrs in both hemispheres, and (3) total observation-impact is reduced, as both 24 hr and 30 hr error-norms are reduced with larger reduction in the 30 hr error-norm.

In TOBS, as in UVTOBS, the impact of all regular observation types is reduced as a result of assimilating pseudo-raobs (Fig. 8), and the largest observation impact is provided by ECMWF pseudo-raob observations. As a percentage of their impact in the Control, high-latitude satellite winds from AVHRR (AVHRR-WIND) are reduced by 55.9 percent, more than any other observation type (Fig. 8b). Other high-latitude satellite wind data (MODIS-WIND, LEO-GEO-WIND) also show substantial impact reductions in TOBS, losing roughly 38 percent of their impact vs. Control. Satellite winds from geostationary imagery (CLD-WIND) lose 27.1 percent of their impact, though reductions

in observation-impact are heavily concentrated in the most poleward southern hemispheric latitudes where geostationary satellite winds are provided (Fig. 8c).

It is hypothesized that a significant portion of observation impact from satellite wind observations assimilated at high latitudes in the southern hemisphere results from the ability of these data to establish analysis wind *and* temperature fields even when the model background temperature is biased. In contrast, assimilation of radiance observations has less potential to correct background temperature bias. In this scenario, we should expect to see large reduction of satellite wind observation-impact when ECMWF pseudo-raob temperature data are assimilated, since the pseudo-raobs are even more effective than satellite wind data at correcting temperature bias that may exist in the NAVGEM analysis. These changes in observation impact and NAVGEM temperature bias are found in results of the TOBS and UVTOBS experiments.

Another approach to investigate evidence of a warm bias in the NAVGEM analysis is to see what, if any, impact from ECMWF pseudo-raobs might persist in the analysis cycle after pseudo-raobs have been continuously assimilated for some period of time, and are then removed from subsequent assimilation. We may expect the impact from the pseudo-raobs to persist for some time, assuming that their effect at previous times continue to propagate through the background forecast (having corrected the warm bias). This experiment is referred to as DIEOFF, described in the next section.

### *3.3) DIEOFF Experiment*

The DIEOFF experiment is initialized on 0000 UTC 20 April 2013, as are the other experiments and the Control simulation. Pseudo-raob wind and temperature profiles

are assimilated, identical to the UVTOBS experiment, from 0000 UTC 20 April 2013 to 1800 UTC 13 May 2013, roughly halfway through the period covered by the previous experiments. Beginning on 0000 UTC 14 May 2013, no additional pseudo-raobs are made available, forcing the data assimilation system to use only the observations available in the Control from that time forward, through 1200 UTC 4 June 2013. After 0000 UTC 14 May 2013, the DIEOFF analyses and forecasts can differ from the Control only through the influence of differences in the model background state for the 0000 UTC 14 May 2013 analysis, which was produced from cycling pseudo-raobs for the previous 23 days. The remainder of the experiment is divided into three phases representing: (i) the first 29 analysis cycles after pseudo-raobs are no longer assimilated (0000 UTC 14 May 2013 – 0000 UTC 21 May 2013), (ii) the next 29 analysis cycles (0600 UTC 21 May 2013 – 0600 UTC 28 May 2013) and (iii) the final 29 analysis cycles (1200 UTC 28 May 2013 – 1200 UTC 04 June 2013). These are referred to as the early, middle, and late phases of the experiment, respectively, which are evaluated separately to illustrate the time-evolution of the experiment as the analysis is cycled without pseudo-raobs and their effect fades.

In the early phase, the difference in the mean analysis 500 hPa height between DIEOFF and the Control (Fig. 9 a) is similar to the differences between UVTOBS and Control (Fig. 10a), with NAVGEM heights lowered globally and largest height reductions found at high latitudes in the southern hemisphere. The analysis temperature differences in DIEOFF (Fig. 9b) are likewise similar to differences in UVTOBS (Fig. 10b) with cooling throughout the lower to mid troposphere and warming aloft. Some effects of psudo-raobs have already begun to fade in the early phase of DIEOFF, with

maximum (negative) height differences only 22 percent of what was observed in UVTOBS over the same period. These height differences continue to diminish in the middle (Fig. 9c,d) and late phases (Fig. 9e,f) of the DIEOFF experiment, especially in the northern hemisphere, while they remain largely unchanged in the UVTOBS experiment over the same time intervals (Fig. 10c-f). By the late period of DIEOFF, the southern hemisphere retains maximum (negative) height differences 10 percent the size of what was observed in UVTOBS (Fig. 10e,f), still concentrated in the southern hemispheric high-latitudes. The maximum reduction in NAVGEM zonal-mean temperature in the southern hemisphere is 18.6 percent of what was observed in UVTOBS in the early phase of the DIEOFF experiment, although this diminishes in the late phase to just 6.8 percent of that in UVTOBS.

About 5 to 10 percent of beneficial pseudo-raob impact on the NAVGEM forecast from UVTOBS is still present in southern hemispheric geopotential height RMS scores during the late period of DIEOFF (Fig. 11d), which follows 58 analysis cycles without pseudo-raob observations. The results here demonstrate that information in the model background from previous cycling of pseudo-raobs can have positive impacts on the forecast even when no new pseudo-raobs are being assimilated. However, almost all positive impact on wind speed RMS errors in the tropics that was observed in UVTOBS is erased by the late period of DIEOFF (Fig. 11f), and geopotential height RMS in the northern hemisphere in DIEOFF is degraded to statistical significance at 120 hr in the upper troposphere (Fig. 11b).

The reduction of 24 hr and 30 hr error-norms in DIEOFF quickly fades within the first eight cycles in the early phase (Fig. 12), though some non-zero impact on the error-

norm remains even into the late phase. The reduction in error-norm is always larger for the 30 hr error-norm than the 24 hr error norm, resulting in reduced total observation impact, with a mean reduction in observation impact in the late phase that is roughly 6.5 percent of that in UVTOBS over the same time period. The largest percentage decrease in observation-impact in the late phase of DIEOFF comes from high-latitude satellite winds (AVHRR-WIND), which lose roughly 7 percent of their impact relative to the Control over the same time period (not shown).

# 4. Conclusions

A set of experiments with the NAVDAS-AR/NAVGEM analysis and forecast system was performed to simulate an improvement to the system through assimilation of high quality synthetic observations. Synthetic wind and temperature observations derived from the ECMWF analysis are assimilated in the NAVDAS-AR as "pseudo-raob" profiles. Assimilation of psuedo-raob profiles improves NAVGEM analyses and forecasts over the global domain, with the most significant improvements (as measured by temperature bias reduction in the analysis and reduction of geopotential height RMS error in the forecast) appearing in the southern hemisphere. Assimilation of pseudo-raob profiles in NAVGEM leads to a cooling of low- to mid-tropospheric temperatures and subsequent lowering of mid-tropospheric geopotential heights, with the largest changes occurring at high latitudes in the southern hemisphere. The analysis changes translate into forecast improvements globally, with statistically significant impacts on hemispheric geopotential height RMS error and tropical wind speed RMS error out to 72-96 hr.

Diagnostic information from the NAVGEM adjoint system illustrates that assimilation of pseudo-raob profiles *reduces* total observation impact, which corresponds to general improvement of NAVGEM analyses and forecasts, including improvement of background forecasts used in data assimilation. When pseudo-raob profiles are assimilated in NAVGEM, they contribute more to reduction of 24 hr forecast error than any other type of data. In addition, use of pseudo-raob data reduces observation impact for all categories of routinely assimilated observatios, with largest impact reductions occurring for satellite-derived wind observations. However, since the added impact from pseudo-raobs is smaller than the reduction of impact from routinely assimilated observations, the *total* observation impact decreases in these experiments. With pseudo-raob assimilation there is reduction of forecast error-norms on both the analysis and background trajectories, but forecast error is reduced to a greater extent on the background trajectory, which corresponds to a reduction of total observation-impact and smaller correction of the background by the data assimilation procedure. This demonstrates that providing more-accurate information such as additional real or synthetic observations to an analysis-forecast system actually reduces the total impact of observations, through convergence of the background and analysis state trajectories.

Comparison of results from the UVTOBS and TOBS experiments illustrates that addition of high-quality wind and temperature information (in this case, from pseudo-raob profiles) can substantially reduce analysis temperature bias in regions where assimilation of existing radiation observations is not effective at removing bias that may exist in the background forecast. This result appears at high latitudes in the southern hemisphere where, in NAVGEM, large observation-impact from satellite wind

observations (in Control) appear to be, at least in part, due to correction of a tropospheric warm bias that is not removed by assimilation of radiance data. In these experiments the assimilation of pseudo-raob information reduces temperature bias in NAVGEM, thereby diminishing the impact of satellite wind observations. Impact of radiation data is also reduced by assimilation of pseudo-raob information, but to a lesser extent, since the accompanying reduction of background temperature bias compensates by making assimilation of regular radiation data more beneficial.

The experiment results also demonstrate a noticeable residual benefit from assimilation of ECMWF pseudo-raobs that persists for several weeks. In the DIEOFF experiment the NAVGEM analyses and forecasts retain some cooling (improvement) of temperatures in the southern hemisphere lower and middle troposphere with modest warming aloft and lowering of 500 hPa geopotential heights even after 58 analysis cycles with no ECMWF pseudo-raobs. There is some improvement in southern hemispheric geopotential height RMSE in forecasts out to 120 hr, while error-norms for the 24 hr and 30 hr forecasts are likewise slightly reduced.

The pseudo-raob assimilation experiments described in this study are diagnostic in character, since it is not practical in real-time operations to obtain or assimilate analysis information from other model systems. In this diagnostic context, however, pseudo-raob experiments are a useful tool to identify aspects of model analyses and forecasts that might be improved, such as bias and observation impact. While this study shows that assimilation of pseudo-raob profiles (derived from ECMWF analysis information) improves NAVGEM analyses and forecasts in an experimental context, it should be noted that products of other model systems would be improved to varying

extents, as long as the assimilated pseudo-raob information, from whatever source, is more accurate than the background used for the data assimilation procedure.

## 5. Acknowledgements

This research was funded with support from the Office of Naval Research, the Naval Research Laboratory, and the Cooperative Institute for Meteorological Satellite Studies. Funding coordination was provided by Chris Velden, Jeffrey Hawkins and Nancy Baker. Computational resources were provided by The Navy DOD Supercomputer Resource Center. Patricia M. Pauley provided assistance with code to assimilate pseudo-raob data in NAVGEM.

# References

Cardinali, C. 2009. Monitoring the observation impact on the short-range forecast. *Quart. J. Roy. Meteor. Soc.*, **135**, 239-250.

Derber, J. C., and Wu, W.-S. 1998. The use of TOVS cloud-cleared radiances in the NCEP SSI Analysis System. *Mon. Wea. Rev.*, **126**, 2287-2299.

Gelaro, R., Langland, R. H., Pellerin, S., and Todling, R. 2010. The THORPEX observation impact intercomparison experiment. *Mon. Wea. Rev.*, **138**, 4009-4025.

Goerss, J. S., and Jeffries, R. A. 1994. Assimilation of synthetic tropical cyclone observations into the Navy Operational Global Atmospheric Prediction System. *Wea. Forecasting*, **9**, 557-576.

Harris, B. A., and Kelly, G. 2001. A satellite radiance-bias correction scheme for data assimilation. *Quart. J. Roy. Meteor. Soc.*, **127**, 1453-1468.

Hogan, T. F., and Rosmond, T. E. 1991. The description of the Navy Operational Global Atmospheric Prediction System's spectral forecast model. *Mon. Wea. Rev.*, **119**, 1786-1815.

Langland, R. H., and Baker, N. L. 2004. Estimation of observation impact using the NRL atmospheric variational data assimilation adjoint system. *Tellus*, **56A**, 189-201.

Langland, R. H., Maue, R. N., and Bishop, C. H. 2008. Uncertainty in atmospheric temperature analyses. *Tellus*, **60A**, 598-603.

Rosmond, T. E., 1997. A technical description of the NRL adjoint modeling system. NRL/MR/7532/97/7230, NRL, 62 pp. [Available from the Naval Research Laboratory, Monterey, CA 93943-502].

Rosmond, T. E., and Xu, L. 2006. Development of NAVDAS-AR: non-linear formulation and outer loop tests. *Tellus A*, **58**, 45-58.

Xu, L., Rosmond, T. E., and Daley, R. 2005. Development of the NAVDAS-AR: formulation and initial tests of the linear problem. *Tellus A*, **57**, 546-559.

Zhu, Y., and Gelaro, R. 2008. Observation sensitivity calculations using the adjoint of the Gridpoint Statistical Interpolation (GSI) analysis system. *Mon. Wea. Rev.*, **136**, 335-351.

# Tables

**Table 1**. Observation types assimilated in the NAVDAS-AR, the observed variables, and the reference name they are given in figures and text. Variables include zonal wind (U), meridional wind (V), temperature (T), pressure (P), specific humidity (Q), as well as others.

| Reference Name | Observation Type | Variable(s) |
|---|---|---|
| AIREP | Routine air report from aircraft | U, V |
| AMDAR | Automated report from Aircraft Meteorological Data Relay | U, V, T |
| AMSU-A | Remote sensing observations from the Advanced Microwave Sounding Unit-A | Brightness Temperature |
| AQUAS | Remote sensing observations from NASA Aqua satellite | Brightness Temperature |
| ASCAT-SFC-WIND | Advanced scatterometer surface wind observations | U, V |
| ATMSS | Remote sensing observations from the Advanced Technology Microwave Sounder | Brightness Temperature |
| AVHRR-WIND | Atmospheric Motion Vectors from the Advanced Very High Resolution Radiometer | U, V |
| CLD-WIND | Atmospheric Motion Vectors from geostationary satellite imagery | U, V |
| ECMWF-PROF | Pseudo-raob profiles from ECMWF analysis | U, V, T |
| GPSMET-R-O | Atmospheric profiles from Global Positioning Satellite Radio Occultation | Refractivity |
| IASIS | Remote sensing observations from the Infrared Atmospheric Sounding Inferometer | Brightness Temperature |
| LandSfc | Land surface observations | U, V, T, P, Q, Height |
| LEO-GEO-WIND | Atmospheric Motion Vectors from combined low-earth-orbiting / geostationary imagery | U, V |
| MDCRS | Aircraft observations from the Meteorological Data Collection and Reporting System | U, V, T |
| MHS | Remote sensing observations from the Microwave Humidity Sounder | Brightness Temperature |
| MODIS-WIND | Atmospheric Motion Vectors from the Moderate Resolution Imaging Spectroradiometer | U, V |
| RADIOSONDE | Rawinsonde balloon observations | U, V, T, P, Q, Height |
| ShipSfc | Surface observations from ships and buoys | U, V, T, P, Q, Height |
| SSMI-SFC-WIND | Surface wind speed observations from the Special Sensor | Wind Speed |

| | | |
|---|---|---|
| | Microwave Imager | |
| SSMIT | Remote sensing observations from the Special Sensor Microwave Imager | Brightness Temperature |
| SSMI-TPW | Total Precipitable Water observations from the Special Sensor Microwave Imager | Total Precipitable Water |
| TC-SYN | Synthetic profile observations derived for tropical cyclone initialization | U, V, P, Height |
| WSAT-SFC-WIND | Ocean surface winds from WindSat | U, V |
| WINDSAT-TPW | Total Precipitable Water observations from Windsat | Total Precipitable Water |

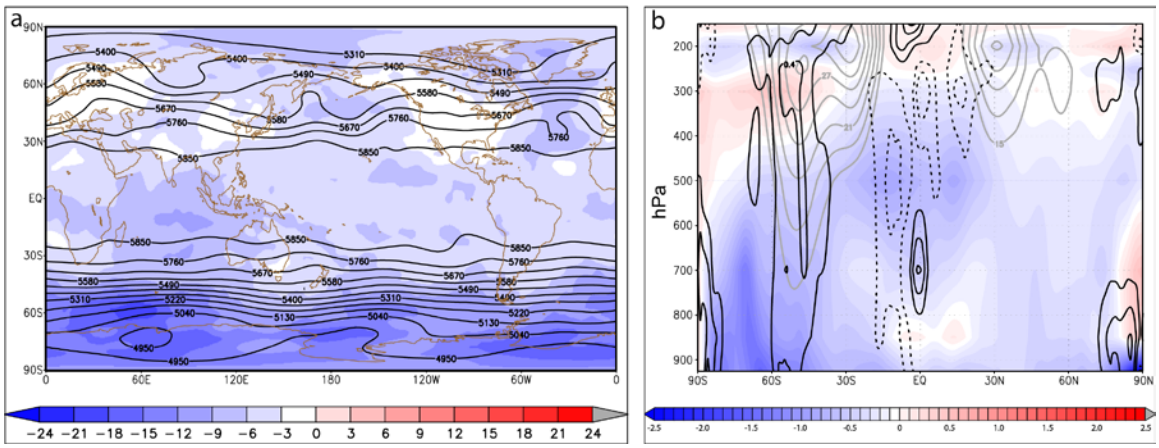


**Figure 1**. Mean analysis differences (UVTOBS – Control) for all analyses (00Z, 06Z, 12Z, and 18Z) from 0000 UTC 20 April 2013 to 1200 UTC 6 June 2013. (a) Difference in 500 hPa geopotential heights shaded every 3 m (cool colors negative), with mean 500 hPa geopotential heights from the Control (black contours every 90 m). (b) Difference in zonal-mean temperature shaded every 0.1 K (cool colors negative), average zonal-mean wind speed from the Control (gray contours every 3 $ms^{-1}$ starting at 15 $ms^{-1}$, and difference in zonal-mean wind (black contours every 0.2 $ms^{-1}$, negative contours dashed).

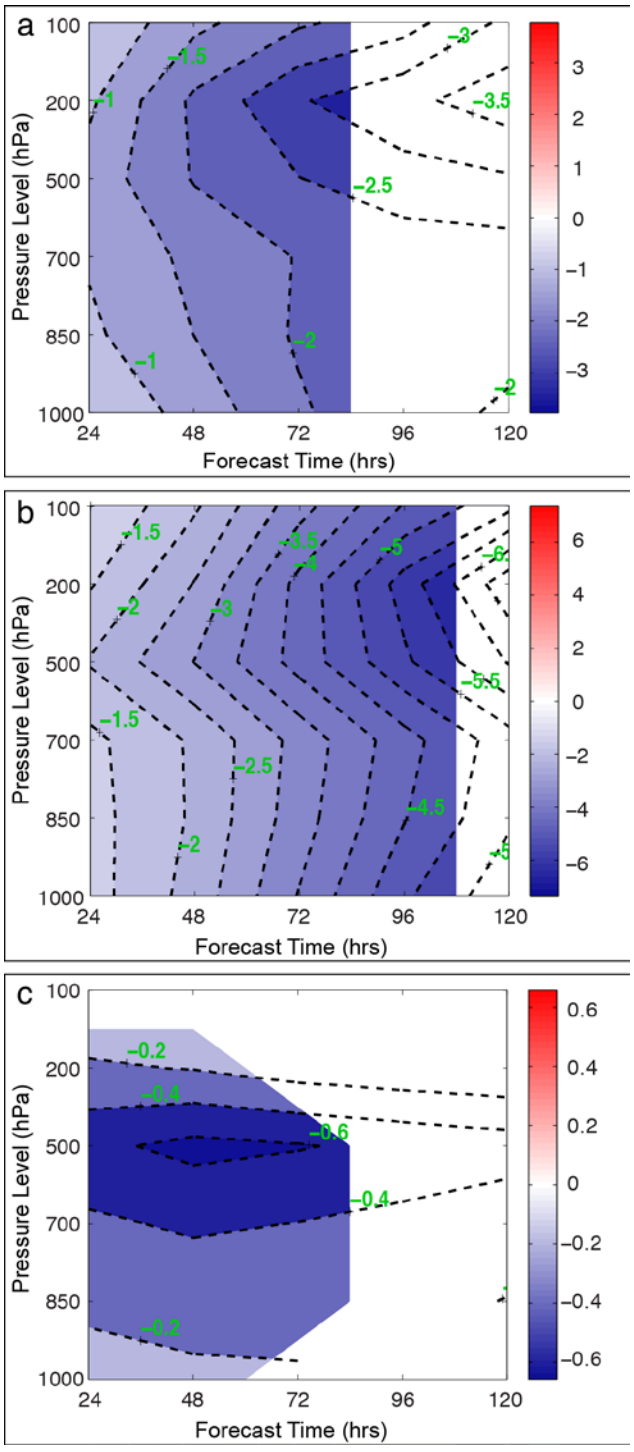


**Figure 2**. Time-pressure plot of difference in mean: (a) northern hemisphere geopotential height RMS (m), (b) southern hemisphere geopotential height RMS (m), and (c) tropical wind speed RMS ($ms^{-1}$) for UVTOBS – Control. Results based on forecasts from 0000 UTC and 1200 UTC from 20 April 2013 – 6 June 2013. Dashed lines provide values at all levels and forecast times, and shading represents where the value passes a student's t-test at 95% confidence.

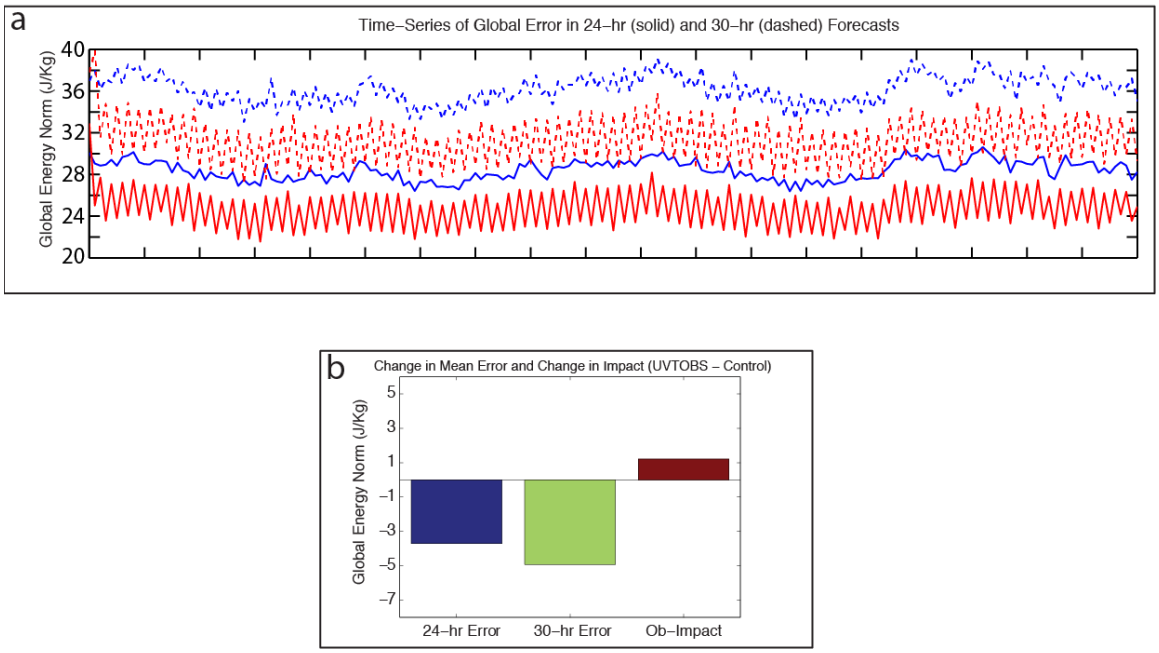


**Figure 3**. (a) Time-series of Control 24 hr error-norm (blue solid), Control 30 hr error-norm (blue dashed), UVTOBS 24 hr error norm (red solid), and UVTOBS 30 hr error-norm (red dashed). (b) Mean difference (UVTOBS – Control) in 24 hr error-norm (blue), 30 hr error-norm (green), and total ob-impact defined as the difference between the 24 hr error-norm and the 30 hr error-norm (red). Error norms are provided for forecasts initialized at 00Z, 06Z, 12Z, and 18Z from 20 April 2013 – 6 June 2013.

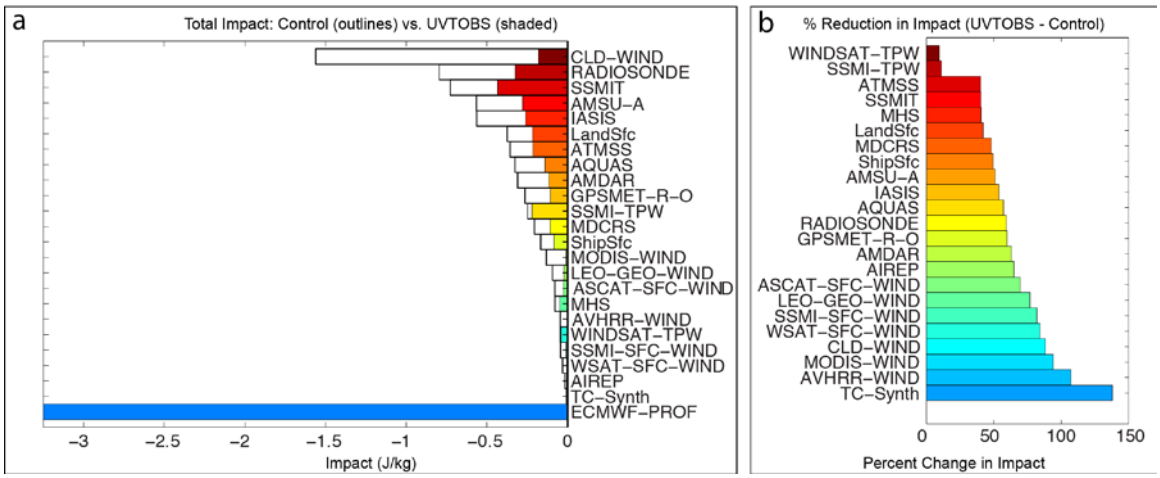


**Figure 4**. (a) Mean observation-impact (J $kg^{-1}$) summed over observation types for the Control (black outline of bars) and UVTOBS (filled portion of bars). The impact of ECMWF pseudo-raobs is shown by the blue bar. Negative values indicate a reduction in 24 hr forecast error from assimilation of the observation type. (b) Percent change in observation-impact (UVTOBS vs. Control) for observation categories. Values less than 100% indicate lower observation impact in UVTOBS. Mean impact is computed for all forecasts initialized 00Z, 06Z, 12Z, and 18Z between 0000 UTC 22 April 2013 – 1200 UTC 6 June 2013.

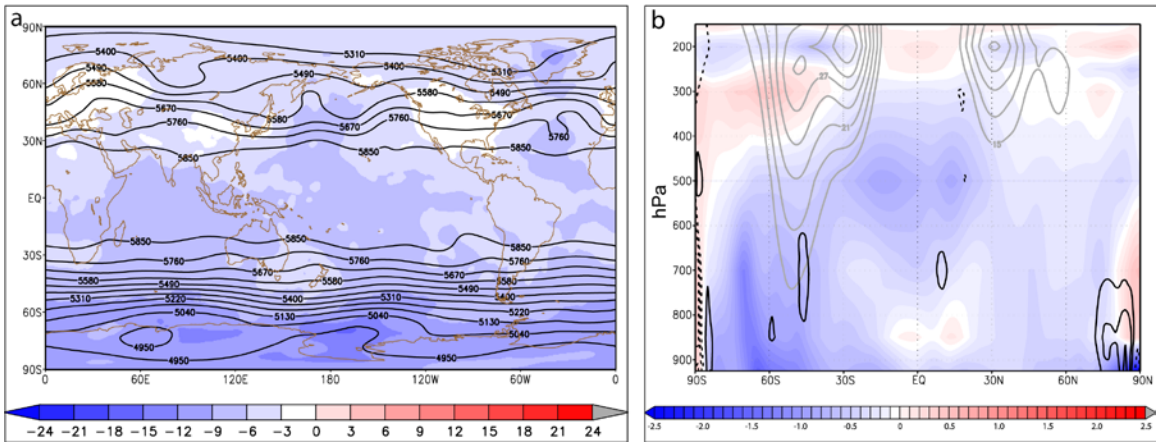


**Figure 5**. Mean analysis differences (TOBS – Control) for all analyses (00Z, 06Z, 12Z, 18Z) from 0000 UTC 20 April 2013 to 1200 UTC 6 June 2013. (a) Difference in 500 hPa geopotential heights shaded every 3 m (cool colors negative), with mean 500 hPa geopotential heights from the Control (black contours every 90 m). (b) Difference in zonal-mean temperature shaded every 0.1 K (cool colors negative), average zonal-mean wind speed from the Control (gray contours every 3 $ms^{-1}$ starting at 15 $ms^{-1}$, and difference in zonal-mean wind (black contours every 0.2 $ms^{-1}$, negative contours dashed).

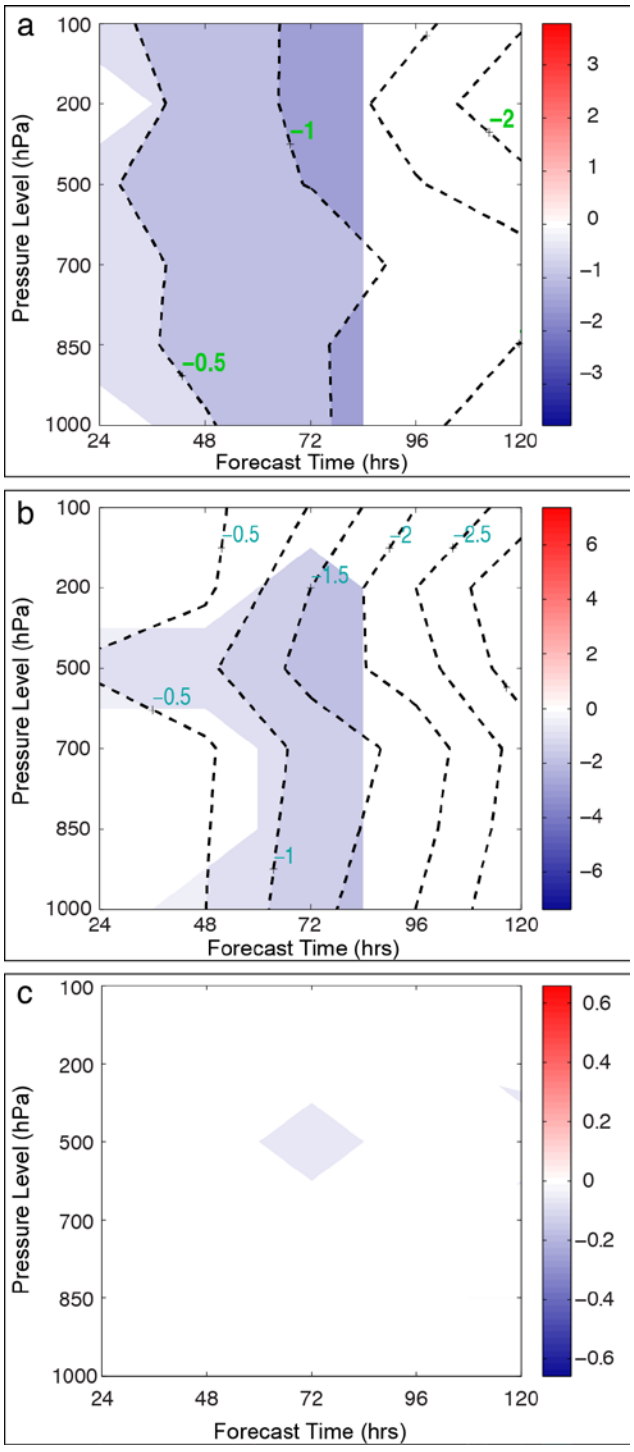


**Figure 6**. Time-pressure plot of difference in mean: (a) northern hemisphere geopotential height RMS, (b) southern hemisphere geopotential height RMS (m), and (c) tropical wind speed RMS ($ms^{-1}$) for TOBS – Control. Results based on forecasts from 0000 UTC and 1200 UTC from 20 April 2013 – 6 June 2013. Dashed lines provide values at all levels and forecast times, and shading represents where the value passes a student's t-test at 95% confidence.

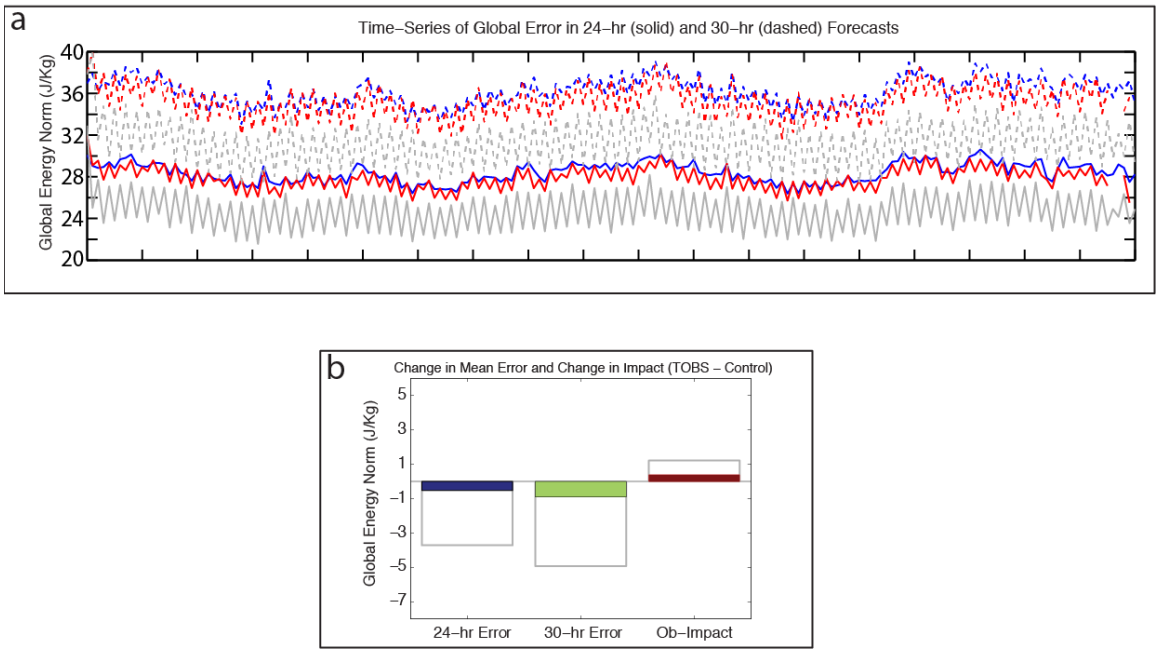


**Figure 7**. (a) Time-series of Control 24 hr error-norm (blue solid), Control 30 hr error-norm (blue dashed), TOBS 24 hr error norm (red solid), and TOBS 30 hr error-norm (red dashed). The time-series of UVTOBS 24 hr error-norm (gray solid) and UVTOBS 30 hr error-norm (gray dashed) are provided for comparison. (b) Filled portion of bars represents the mean difference (TOBS – Control) in 24 hr error-norm (blue), 30 hr error-norm (green), and total ob-impact defined as the difference between the 24 hr error-norm and the 30 hr error-norm (red). The corresponding values for (UVTOBS – Control) are provided as gray outlines for reference. Error norms are provided for forecasts initialized at 00Z, 06Z, 12Z, and 18Z from 20 April 2013 – 6 June 2013.

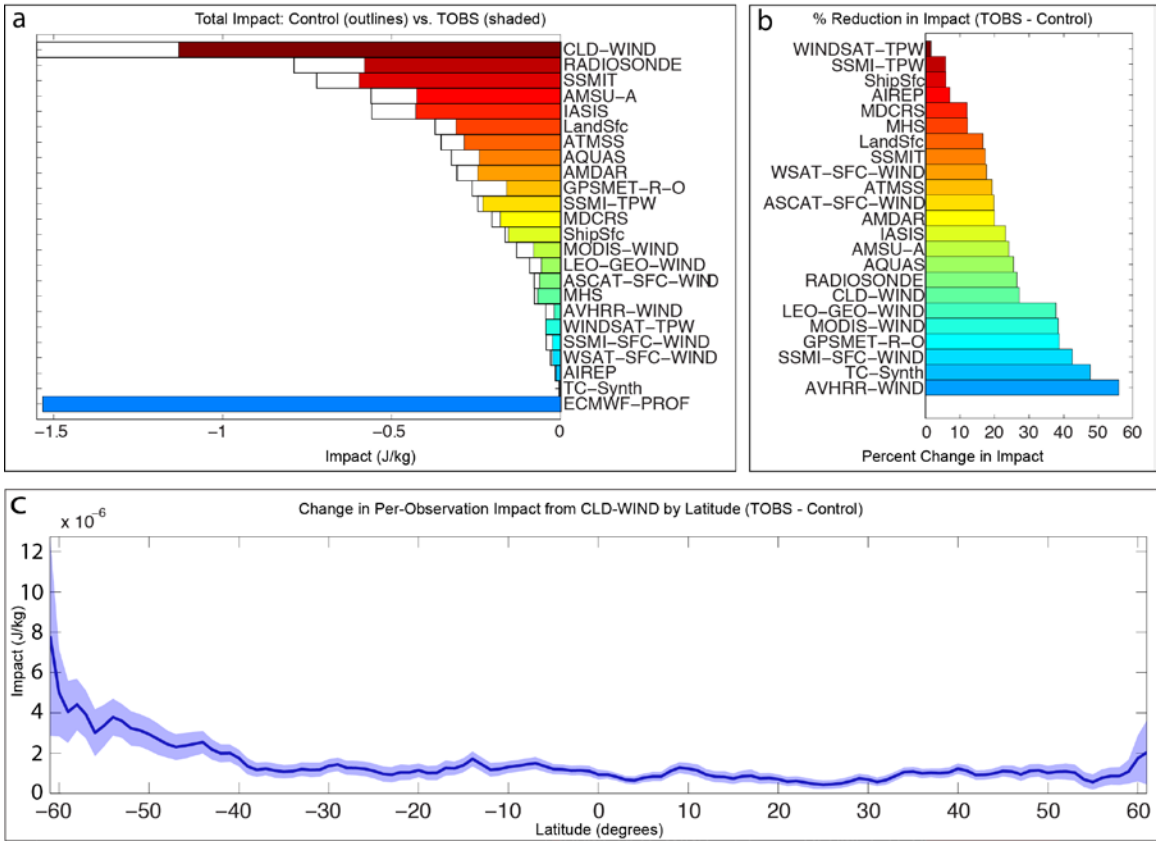


**Figure 8**. (a) Mean observation-impact (J $kg^{-1}$) summed over observation types for the Control (black outline of bars) and TOBS (filled portion of bars). The impact of ECMWF pseudoraobs is provided in the blue bar. Negative values indicate a reduction in 24 hr forecast error from assimilation of the observation type. (b) Percent change in observation-impact (TOBS vs. Control) for observation categories. Values less than 100% indicate lower observation impact in TOBS. (c) Difference (TOBS – Control) in mean per-observation CLD-WIND observation-impact averaged by latitude. Solid blue line represents the mean value, shading represents 95% confidence limits on the mean. Mean impact is computed for all forecasts initialized 00Z, 06Z, 12Z, and 18Z between 0000 UTC 22 April 2013 – 1200 UTC 6 June 2013.

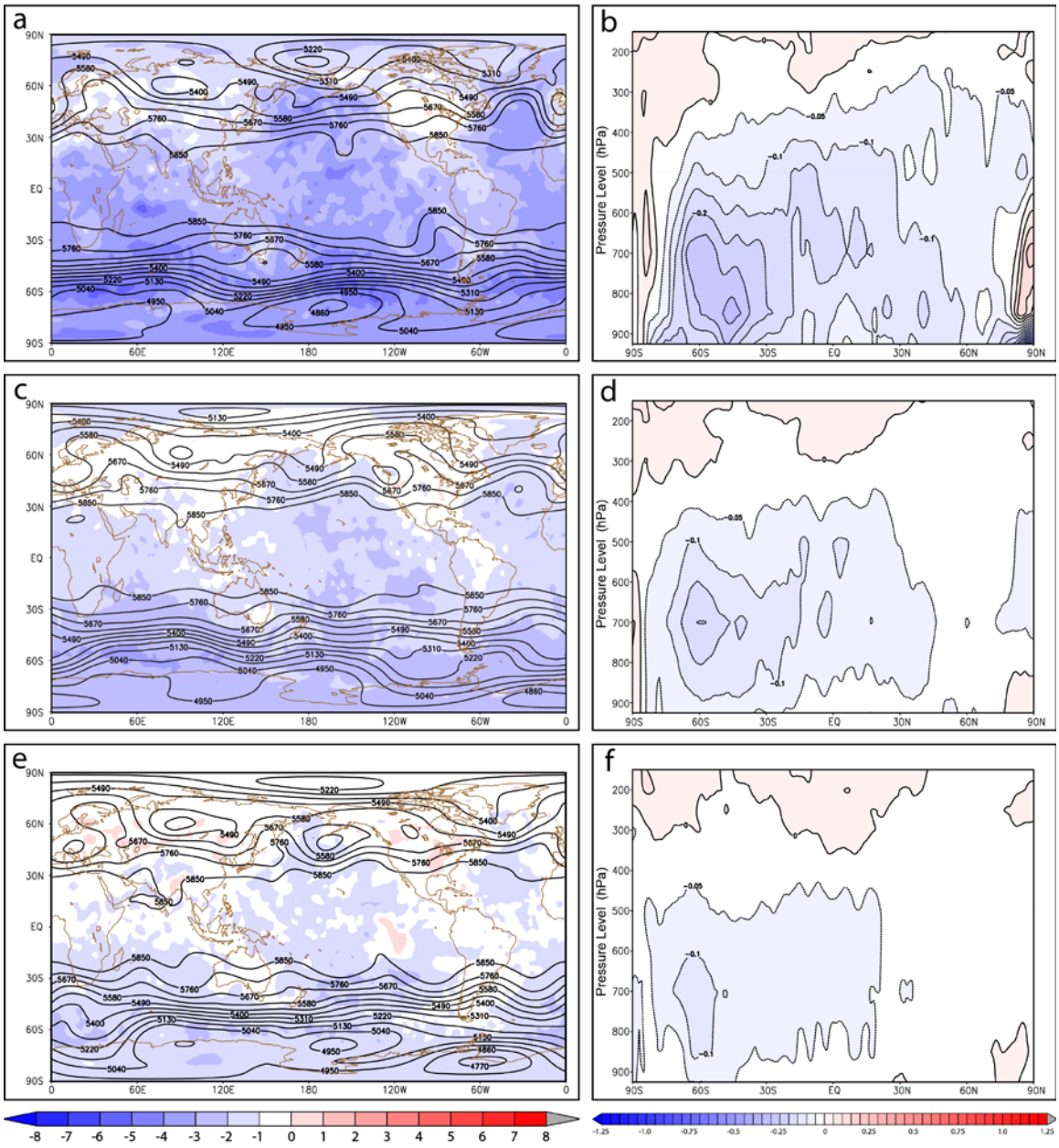


**Figure 9**. Mean analysis differences (DIEOFF – Control) for three sequential 29 analysis cycle periods: the early period from 0000 UTC 14 May 2013 – 0000 YTC 21 May 2013 (panels a, b), the middle period from 0600 UTC 21 May 2013 – 0600 UTC 28 May 2013 (panels c, d), and the late period from 1200 UTC 28 May 2013 – 1200 UTC 04 June 2013 (panels e, f). Left panels are mean geopotential height differences at 500 hPa (shaded every 1 m, cool colors negative) and mean geopotential heights from the Control (black contours every 90 m). Right panels are mean zonal-average temperature differences by latitude and pressure level, shaded and contoured every 0.05 K.

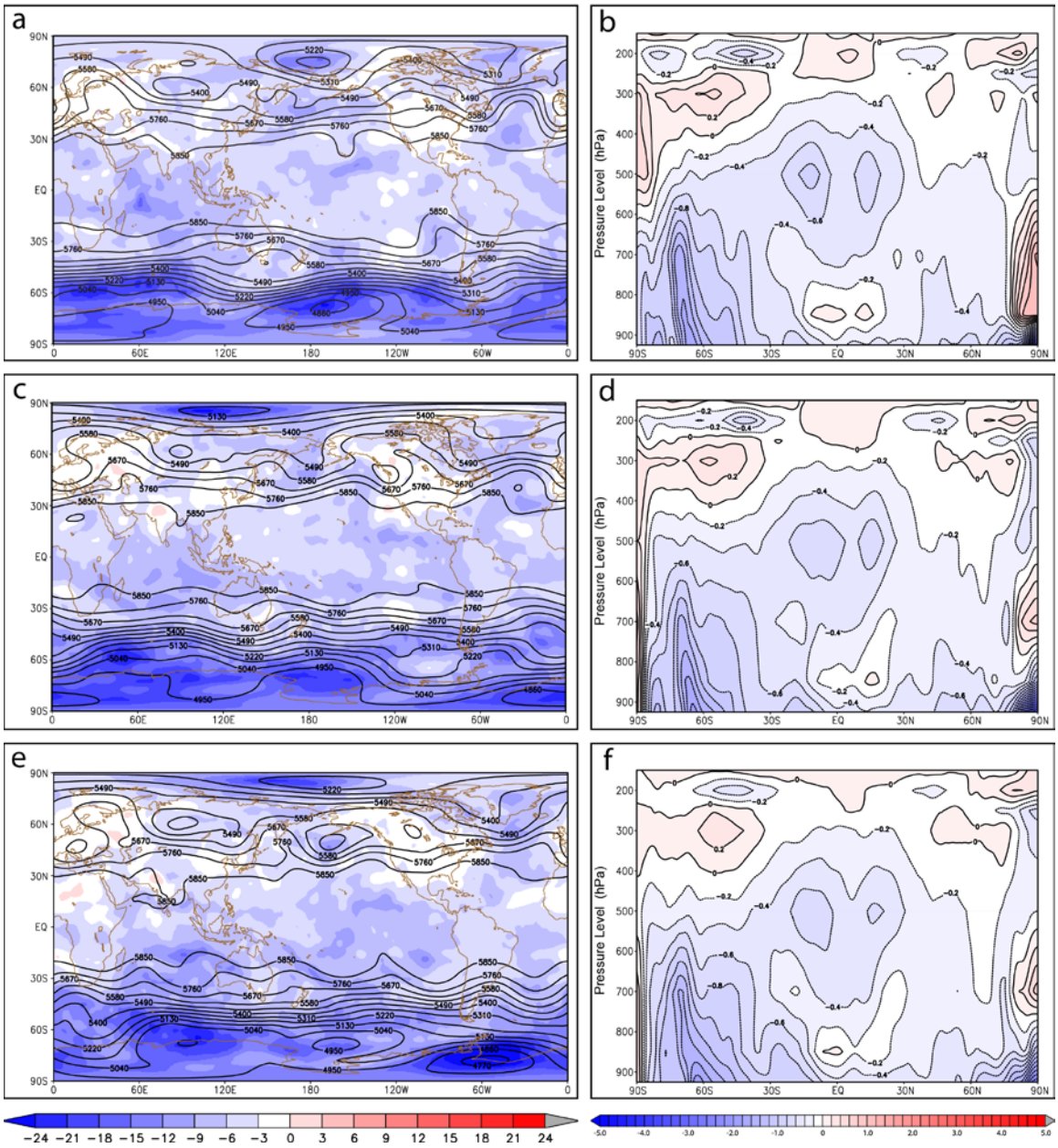


**Figure 10**. As in Figure 9, but for (UVTOBS – Control). Geopotential height differences in a,c,e are shaded every 3 m (cool colors negative), and zonal-average temperature differences in b,d,f are shaded and contoured every 0.2 K (cool colors negative).

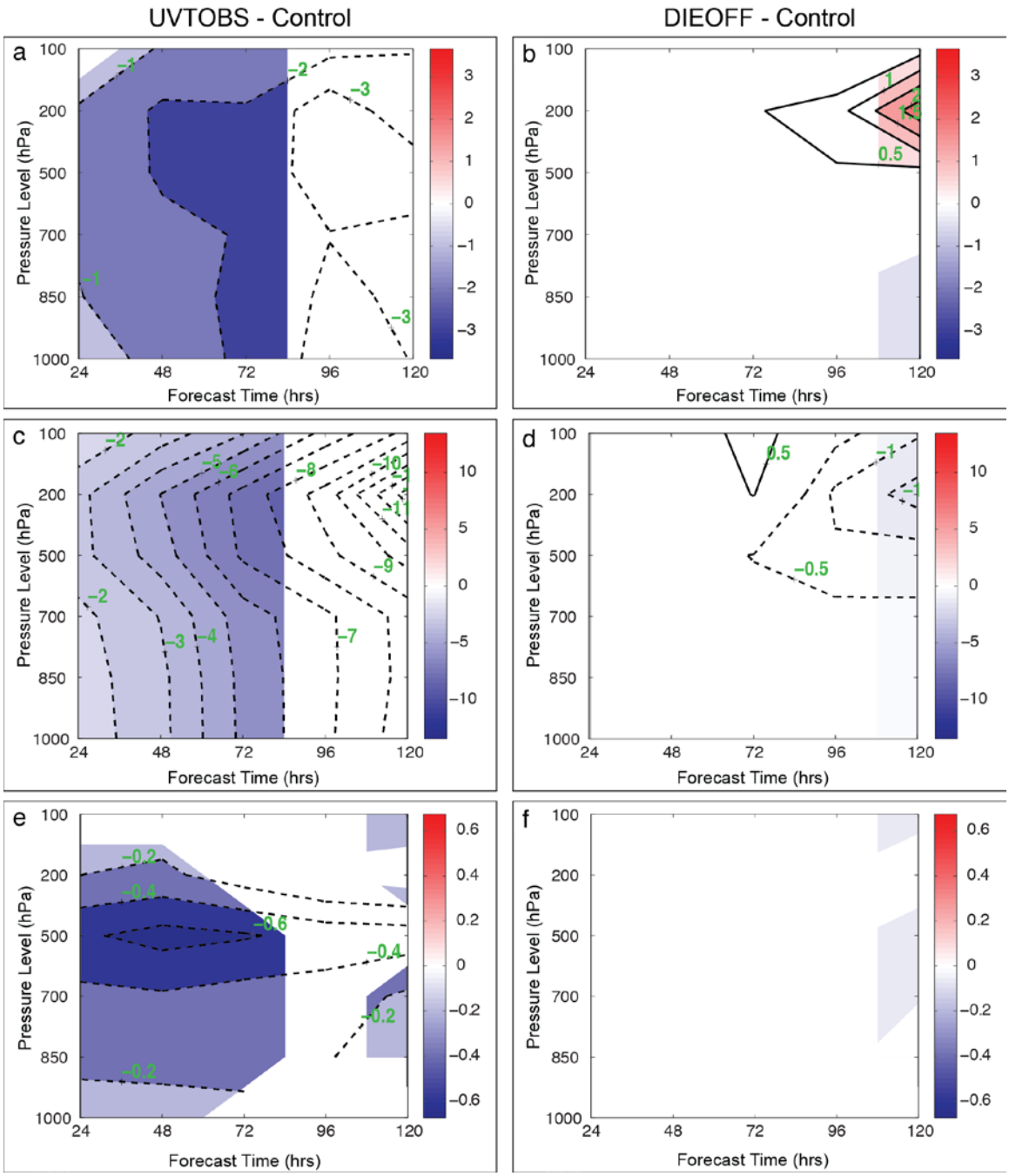


**Figure 11**. Time-pressure plot of difference in mean: (a,b) northern hemisphere geopotential height RMS, (c,d) southern hemisphere geopotential height RMS, and (e,f) tropical wind speed RMS for (left panels) UVTOBS – Control, and (right panels) DIEOFF – Control, averaged using forecasts initialized at 0000 UTC and 1200 UTC during the late period from 1200 UTC 28 May 2013 – 1200 UTC 04 June 2013. Dashed lines provide values at all levels and forecast times, and shading represents where the value passes a student's t-test at 95% confidence. Note that contour intervals for the right panels are at twice the resolution of contour intervals for the left panels.

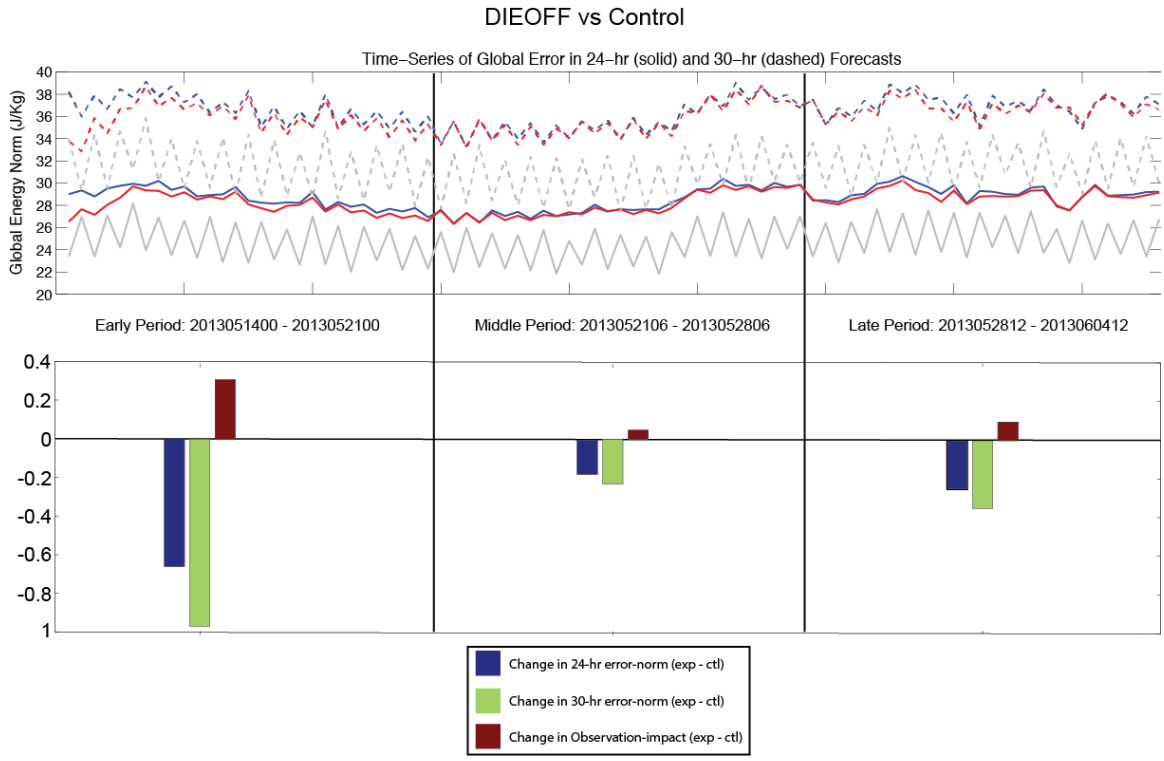


**Figure 12**. (Top) Time-series of Control 24 hr error-norm (blue solid), Control 30 hr error-norm (blue dashed), DIEOFF 24 hr error norm (red solid), and DIEOFF 30 hr error-norm (red dashed). The timeseries of UVTOBS 24 hr error-norm (gray solid) and UVTOBS 30 hr error-norm (gray dashed) are provided for reference. (Bottom) Mean difference (DIEOFF – Control) in 24 hr error-norm (blue), 30 hr error-norm (green), and total ob-impact defined as the difference between the 24 hr error-norm and the 30 hr error-norm (red). Bars are computed for the early, middle, and late period separately, centered on their appropriate portion of the time-series demarcated by the vertical black lines.